

CERAMICS, ELECTRONIC PROPERTIES AND MATERIAL STRUCTURE

The properties of a ceramic material that make it suitable for a given electronic application are intimately related to such physical properties as crystal structure, crystallographic defects, grain boundaries, domain structure, microstructure, and macrostructure. The development of ceramics that possess desirable electronic properties requires an understanding of the relationship between material structural characteristics and electronic properties and how processing conditions may be manipulated to control structural features.

1. Properties and Applications

1.1. Insulators

Ceramic insulators are materials used to support electrical conductors and to prevent the flow of electrical charge between them. Ceramic bodies, such as triaxial porcelains based on compositions in the Al_2O_3 – $(\text{K},\text{Na})_2\text{O}$ – SiO_2 phase diagram, were initially employed as high voltage insulators. Since then, other ceramics have been utilized in higher technology insulation applications, eg, in packaging and very large-scale integration (VLSI) circuits (see Integrated circuits). VLSI, or multilayer ceramic (MLC), technology involves cofiring conductor and insulator layers to build-up multilayer electronic modules, thus increasing device, or circuit, density. Alumina, Al_2O_3 , is the material most frequently used for these applications, although because of its very high thermal conductivity, beryllia, BeO , has also been used as a substrate material. Other ceramics, namely, aluminum nitride and glass-ceramics (qv), such as cordierite [12182-53-5] and cordierite/mullite composites, have also been investigated for use in packaging applications (see Packaging, semiconductors and electronic materials). The development of cordierite as a substrate material has progressed to the state where, in conjunction with cosinterable copper electrodes, it is used as the multilayer substrate in high performance computers (see Computer technology).

The usefulness of ceramics for all of these applications is because of their dielectric, or insulating, characteristics. Properties important for insulation applications include: (1) dielectric constant k' : a measure of the ability of a material to store electrical charge; (2) electrical resistivity ρ : the resistance to current flow; (3) dissipation factor or $\tan \delta$; a measure of the energy loss per cycle (in an a-c field); and (4) dielectric breakdown strength (DS): the maximum voltage gradient that can be impressed across the dielectric without destroying its insulating characteristics. So that dielectric loss may be minimized, materials having low (<10) dielectric constants and low (<0.001) dissipation factors are desired for substrate applications.

The observed dielectric constant k' and the dielectric loss factor $k = k' \tan \delta$ are defined by the charge displacement characteristics of the ceramic; ie, the movement of charged species within the material in response to the applied electric field. Discussion of polarization mechanisms is available (1).

Other features of ceramic materials are also important in insulation applications. For example, in packaging applications, not only the electrical properties of Al_2O_3 , but also the thermal conductivity, for heat dissipation, thermal expansion behavior, and mechanical strength are important. Properties of ceramic

2 CERAMICS, ELECTRONIC PROPERTIES AND MATERIAL STRUCTURE

insulators are affected by the composition and processing history of the ceramic body. For example, for triaxial porcelains processed by viscous sintering, the relative amounts of the raw materials used, kaolin and ball clay (primarily $\text{Al}_2\text{O}_3 \cdot 2\text{SiO}_2 \cdot 2\text{H}_2\text{O}$) (see Clays); feldspar, $(\text{K},\text{Na})_2\text{O} \cdot \text{Al}_2\text{O}_3 \cdot 6\text{SiO}_2$; and flint, SiO_2 ; and the time—temperature processing cycle, determine the relative amounts of the resulting phases (mullite, alkali-silica glass, and silica) present.

In contrast to triaxial porcelains, packaging materials such as 99% Al_2O_3 prepared by a solid-state sintering process, display significantly lower dielectric loss. In these materials, there is no residual glassy phase with its associated mobile ion content, and therefore, conduction losses are minimized.

1.2. Capacitors

Ceramic materials suitable for capacitor (charge storage) use are also dependent on the dielectric properties of the material. Frequently the goal of ceramic capacitors is to achieve maximum capacitance in minimum volume. The defining equation for capacitance is given by:

$$C = k' \epsilon_0 \frac{A}{d} \quad (1)$$

where k' is the dielectric constant, ϵ_0 is the permittivity of free space, A is the electrode area, and d is the separation between the electrodes. Whereas the dielectric constant is a fundamental material property, it depends on such factors as temperature, stress, electric field strength, and measurement, or use, frequency. Physical features of the ceramic, such as porosity, grain size, and the presence of grain boundary phases, may also affect the observed dielectric constant. The charge storage capabilities of ceramic capacitors are increased by: (1) using ferroelectric or relaxor ferroelectric materials (see Ferroelectrics); (2) preparing materials having large effective dielectric constants ($k' \sim 10,000 - 60,000$) through control of the electric susceptibilities and resistivities of grain and grain boundary phases, eg, internal boundary layer capacitors (IBLCs); or (3) using a multilayering approach, to prepare a structure having alternating electrode/dielectric layers.

Historically, materials based on doped barium titanate were used to achieve dielectric constants as high as 2,000 to 10,000. The high dielectric constants result from ionic polarization and the stress enhancement of k' associated with the fine-grain size of the material. The specific dielectric properties are obtained through compositional modifications, ie, the inclusion of various additives at different doping levels. For example, additions of strontium titanate to barium titanate shift the Curie point, the temperature at which the ferroelectric to paraelectric phase transition occurs and the maximum dielectric constant is typically observed, to lower temperature as shown in Figure 1 (2).

Because of very high dielectric constants ($k' > 20,000$), lead-based relaxor ferroelectrics, $\text{Pb}(\text{B}_1\text{B}_2)\text{O}_3$, where B_1 is typically a low valence cation and B_2 is a high valence cation, have been investigated for multilayer capacitor applications. Relaxor ferroelectrics are dielectric materials that display frequency dependent dielectric constant versus temperature behavior near the Curie transition. Dielectric properties result from the compositional disorder in the B_1 and B_2 cation distribution and the associated dipolar and ferroelectric polarization mechanisms. Close control of the processing conditions is required for property optimization. Capacitor compositions are often based on lead magnesium niobate (PMN), $\text{Pb}(\text{Mg}_{1/3}\text{Nb}_{2/3})\text{O}_3$, and lead zinc niobate (PZN), $\text{Pb}(\text{Zn}_{1/3}\text{Nb}_{2/3})\text{O}_3$.

Multilayer capacitor devices have become progressively smaller as the dielectric constant of the ceramic layers has increased, and layer thickness has decreased to below $15 \mu\text{m}$. The gain in volumetric efficiency over a standard single-layer, or disk, capacitor ($C/v \sim 2 \mu\text{F}/\text{cm}^3$) may be estimated by assuming a typical multilayer capacitor configuration (50, $15\text{-}\mu\text{m}$ thick, 0.25 cm^2 area dielectric layers having $k' = 10,000$). Using these assumptions, a volumetric efficiency of $230 \mu\text{F}/\text{cm}^3$, or a two-order of magnitude gain in efficiency, is observed. In addition to high volumetric efficiency, these devices also offer high reliability, low cost, and large absolute capacitance.

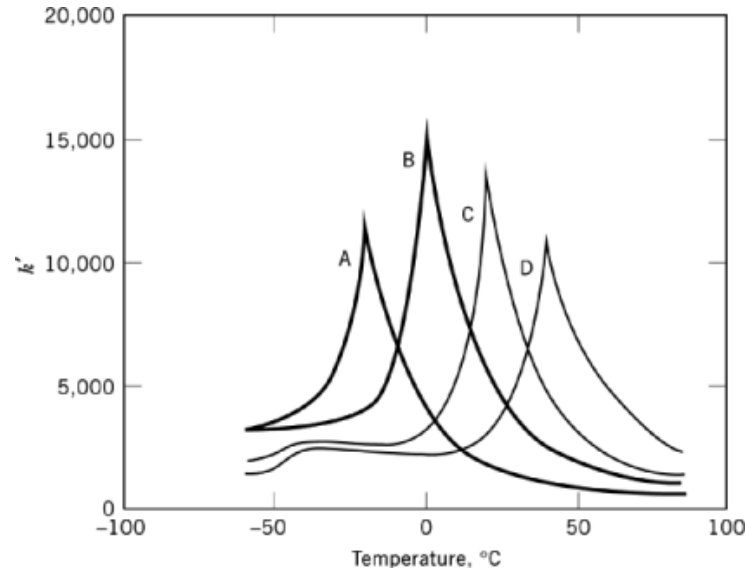


Fig. 1. Effect of compositional variations on the dielectric properties of strontium titanate-barium titanate solid solutions. A, $\text{Ba}_{0.61}\text{Sr}_{0.39}\text{TiO}_3$; B, $\text{Ba}_{0.68}\text{Sr}_{0.32}\text{TiO}_3$; C, $\text{Ba}_{0.74}\text{Sr}_{0.26}\text{TiO}_3$; and D, $\text{Ba}_{0.79}\text{Sr}_{0.21}\text{TiO}_3$ (2).

There is also growing interest in thin-film dielectric capacitors. For example, through the use of processing techniques such as sol-gel solution deposition, thin ($\sim 0.25 \mu\text{m}$) ceramic layers having dielectric constants ranging from 500 to 2000 in the PZT, $\text{Pb}(\text{Zr,Ti})\text{O}_3$, and PMN-PT, $\text{Pb}(\text{Mn}_{1/3}\text{Nb}_{2/3})\text{O}_3$ - PbTiO_3 , compositional families respectively, have been prepared (3).

1.3. Piezoelectrics

All ceramics display a slight change in dimension, or strain, under the application of an electric field. When the induced strain is proportional to the square of the field intensity, it is known as the electrostrictive effect, and is expressed by:

$$S = \xi E^2 \quad (2)$$

where ξ is the electrostrictive coefficient (m^2/V^2) and E is the applied electric field (V/m). Materials that also show the opposite effect, ie, an induced polarization (electric charge) resulting from an applied stress, are referred to as piezoelectric materials, and the effect is referred to as the direct piezoelectric effect. Piezoelectric properties may be described in terms of D , the dielectric displacement; E , the electric field; and T , the applied stress. The direct piezoelectric effect is expressed by:

$$D = dT \quad (3)$$

where d is the direct piezoelectric coupling coefficient expressed in C/N . Piezoelectric materials also display the reverse effect; ie, the development of a strain S in response to an applied electric field (the converse piezoelectric effect):

$$S = d^* E \quad (4)$$

4 CERAMICS, ELECTRONIC PROPERTIES AND MATERIAL STRUCTURE

where d^* is the converse piezoelectric coupling coefficient, expressed in m/V. Generally, the first-order piezoelectric coupling coefficient is much larger than the second-order electrostrictive coefficient, and therefore, for the applications discussed, the piezoelectric response of the material is more important than the electrostrictive response. Although not indicated in the above equations, ξ , d , and d^* are all tensor material properties, and thus are directional in nature.

Certain crystal symmetry requirements are necessary for the existence of piezoelectric behavior in materials. The most widely used class of piezoelectric ceramics possess the ABO_3 perovskite crystal structure, where A is usually a low valence cation and B is a high valence cation. The structure consists of a cubic close packed array of oxygen and A-site ions, and the B-site ions occupy one-fourth of the octahedral interstices that are not adjacent to the A-site ions. Other useful piezoelectrics possess the tungsten bronze, AB_2O_6 , structure.

The piezoelectric electromechanical coupling effects allow for the conversion of mechanical energy into electrical energy or electrical into mechanical energy, thus defining two different classes of transducer applications. Uses range from hydrophones and microphones, to power transducers for ultrasonic cleaning baths. Other applications include filters and resonators. Most (polycrystalline) piezoelectric ceramics for transducer applications are based on compositions in the PZT, $PbZrO_3$ – $PbTiO_3$, family. The materials are used in a polycrystalline form, and to observe the piezoelectric effect, the bulk ceramic must first be uniformly polarized. This is typically accomplished by taking advantage of the ferroelectric nature of PZT and poling after processing (4). PZT compositions near the morphotropic phase boundary are frequently selected not only because they possess high piezoelectric coupling coefficients, but because they are also more easily poled. Other piezoelectric materials that have been employed include quartz, doped $BaTiO_3$, doped $PbTiO_3$, which has been used for acoustic imaging, and PZT-polymer composites, which have been used in hydrophone applications.

1.4. Pyroelectrics

Pyroelectric ceramics are materials that possess a unique polar axis and are spontaneously polarized in the absence of an electric field. Pyroelectrics are also a subset of piezoelectric materials. Ten of the 20 crystal classes of materials that display the piezoelectric effect also possess a unique polar axis, and thus exhibit pyroelectricity. In addition to the induced charge resulting from the direct pyroelectric effect, a change in temperature also induces a surface charge (polarization) from the piezoelectric nature of the material, and the strain resulting from thermal expansion.

Ceramics that display the pyroelectric effect also exhibit a variation in polarization with temperature, as shown in Figure 2. The nature of the temperature variation is dependent on the type of crystallographic transformation that the material displays at the Curie point; ie, whether the transition is first or second order.

The most commercially important application that takes advantage of the pyroelectric effect in polycrystalline ceramics is infrared detection, especially for wavelengths in excess of $2.5\ \mu\text{m}$. Applications range from radiometry and surveillance to thermal imaging, and pyroelectric materials work under ambient conditions, unlike photon detectors, which require cooling.

A second mode of pyroelectric operation is also possible. In addition to the standard pyroelectric mode, where a change in the detector temperature caused by a variation in the incident radiation intensity results in a change in polarization and therefore a current flow as described herein, ferroelectric ceramics may also be operated in a dielectric bolometer mode. Operation in this mode is based on the variation in permittivity ($d\epsilon/dT$) that occurs in the region of the Curie transition (Fig. 3). A change in the detector temperature, arising from a change in the incident radiation level, causes a variation in the permittivity, and when the detector is operated under an applied bias, a voltage output results.

The perovskite ferroelectrics are again the most frequently used ceramics for infrared detector applications. Both single-crystal and polycrystalline materials have been investigated. Single-crystal lithium tantalate, $LiTaO_3$, has been used in single-element detectors. Polycrystalline ceramic devices are frequently based

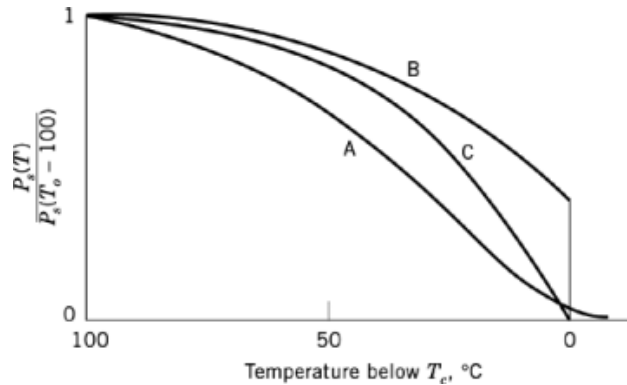


Fig. 2. Polarization plotted as a function of temperature below the Curie transition temperature T_c , for A, relaxors; B, first-order; and C, second-order ferroelectrics (5).

on lead scandium tantalate (for bolometer mode operation), or other lead-based ABO_3 perovskite compositions. Various dopants are added to optimize specific properties, such as pyroelectric coefficient, the Curie transition temperature, permittivity, and dielectric loss. The detector element compositions can become fairly complex with the inclusion of these additives. For example, one material (8) is based on lead zirconium iron niobate (PZFN), but also incorporates titanium and uranium additions to improve the properties, resulting in the following composition: $Pb_{1.02}(Zr_{0.58}Fe_{0.20}Nb_{0.20}Ti_{0.02})_{0.994}U_{0.006}O_3$. The small amount of excess lead is added to improve the sintering behavior of the material.

Single-crystal pyroelectrics are generally prepared by Czochralski growth. Polycrystalline materials are frequently prepared by hot pressing, followed by subsequent thinning and polishing to prepare sections $\sim 10 - 30 \mu m$ in thickness. Multielement arrays are prepared from these sections by selective etching, electroding, and connection to silicon microcircuitry using solder-bump technology. Developments in the sol-gel processing of ferroelectric thin films and sacrificial etching techniques may allow for more straightforward, direct integration of pyroelectric detectors onto silicon devices.

1.5. Ferroelectrics

Ferroelectrics, materials that display a spontaneous polarization in the absence of an applied electric field, also display pyroelectric and piezoelectric behavior. The distinguishing characteristic of ferroelectrics, however, is that the spontaneous polarization must be re-orientable with the application of an electric field of a magnitude lower than the dielectric breakdown strength of the material.

The ferroelectric properties of perovskite materials, and the onset of ferroelectric behavior at a specific temperature, are inherently related to both the domain and crystal structures of the material. For example, in ABO_3 perovskite ferroelectrics, the onset of a macroscopic spontaneous polarization, ie, the spontaneous alignment of dipoles, that is observed on cooling below the Curie temperature is intimately related to a change in the crystal structure occurring at the Curie temperature. As an example, $BaTiO_3$ transforms on cooling from a cubic paraelectric structure to a tetragonal ferroelectric structure at a T_c of $\sim 125^\circ C$. This crystallographic distortion involves ionic displacements that destroy the symmetry of the nonpolar structure, and includes movement of the B-site species to minimum free energy, off-center positions resulting in the generation of permanent electric dipoles in the material, the observed macroscopic spontaneous polarization, and the comparatively high dielectric constants associated with dipolar polarization. Crystallographic and dielectric properties of $BaTiO_3$ are shown in Figure 3.

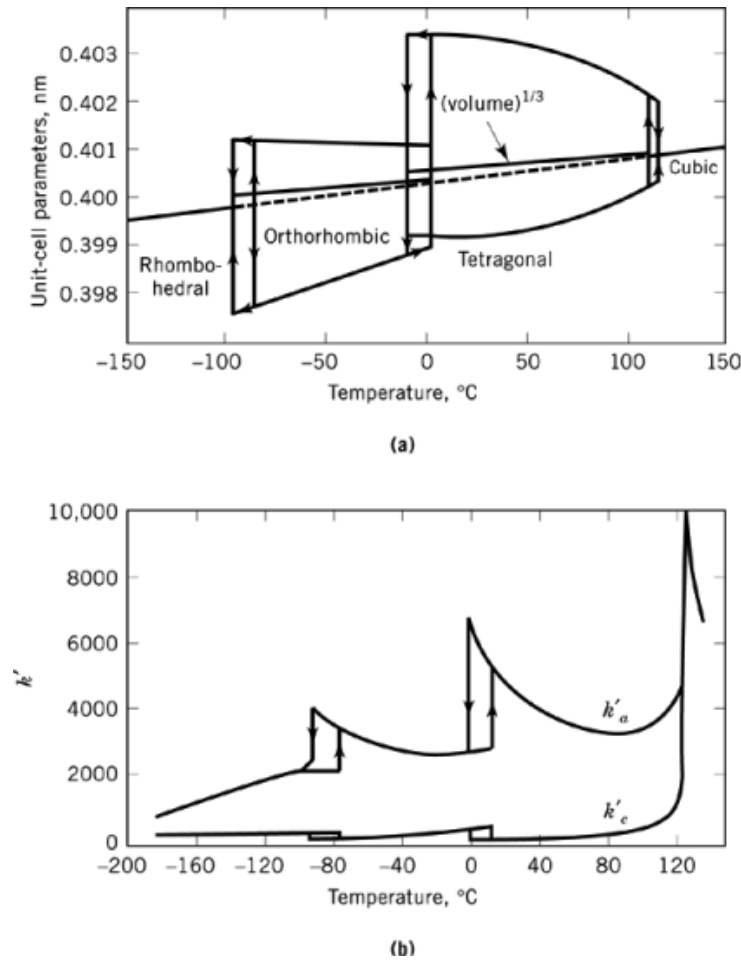


Fig. 3. (a) Crystallographic and (b) dielectric properties of BaTiO₃ as a function of temperature (6, 7).

The number of applications utilizing the ferroelectric response of ceramic materials has been limited. Memory products are under development and are anticipated to be commercially available during the early to mid-1990s.

1.6. Ferrites

Magnetic ceramics or ferrites (qv) may be classified according to crystal structure and the type of magnetic properties: (1) spinel ferrites; (2) hexagonal ferrites, ie, the magnetoplumbites; and (3) rare-earth ferrites, which crystallize in the garnet structure. The garnet materials, so named because they crystallize in the structure of garnet, have the chemical formula $3\text{Me}_2\text{O}_3 \cdot 5\text{Fe}_2\text{O}_3$, where Me is Y or Gd. These rare-earth ferrites are used in microwave devices (see Microwave technology) and bubble memory applications.

Hard materials, so named because they are difficult to demagnetize, are used in permanent magnet applications. The general chemical formula for these materials is $\text{MeO} \cdot 6\text{Fe}_2\text{O}_3$, where Me is a Group 2 (IIA) metal, usually Sr or Ba. The materials crystallize in a hexagonal structure, leading to the name hexagonal ferrites or hexaferrites. They are also isostructural with the naturally occurring mineral, magnetoplumbite.

The most commonly used ferrites, the so-called soft ferrites, are used in soft magnet and low field telecommunication applications, low power transformers, television tube scanning yokes, recording heads, magnetic recording media (see Magnetic tape), antennae, and channel filters. Soft ferrites crystallize in the spinel structure and are characterized by the general formula, MeFe_2O_4 . That is, they consist of a divalent oxide, MeO , typically a transition-metal oxide, such as NiO , CoO , MnO , or ZnO , and iron oxide, Fe_2O_3 . The spinel crystal structure is a cubic AB_2O_4 structure, named for the naturally occurring mineral spinel, MgAl_2O_4 . It consists of cubic close-packed oxygen ions with one-eighth of the tetrahedral sites occupied by divalent Mg , and one-half of the octahedral sites occupied by trivalent Al . Some ferrites also crystallize in the inverse spinel structure, where the divalent cations reside on the B sites, and the trivalent cations are equally split between the A and B sites. Other ferrites, such as MnFe_2O_4 , have an intermediate structure, with $\sim 80\%$ of the manganese ions on the A site and the remaining 20% on the B site. The ferromagnetism of the soft ferrites results from the antiferromagnetic coupling between the cations on the two different crystallographic sublattices.

The existence of solid solutions between different mixed oxides allows for a substantial ability to tailor specific properties. The most common of the soft ferrites is manganese zinc ferrite, $\text{MnFe}_2\text{O}_4\text{--ZnFe}_2\text{O}_4$, and the ability to tailor properties in this system results, in part, from the fact that manganese is paramagnetic whereas zinc is nonmagnetic. A typical ferrite composition also includes other oxide dopants, such as calcia and silica. During processing, these dopants migrate to the grain boundaries, which increases the resistivity of the ferrite, and further minimizes eddy current loss. Because eddy current loss is inversely proportional to frequency, ferrites are well suited to high frequency applications. Other properties that may be tailored through compositional control include coercivity, saturation flux density, and permeability (9).

1.7. Sensors

One growth area for electronic ceramics is in sensor applications. Sensors (qv) are devices that transform nonelectrical inputs into electrical outputs, thus providing environmental feedback. Smart, or intelligent, sensors also allow for mechanisms such as self-diagnosis, recovery, and adjustment for process monitoring and control (see Process control).

Ceramic sensor applications are widely varied and likely to grow in part, because of the increasing emphasis on process control, waste minimization, and environmentally conscious manufacturing. Sensors are used for the measurement of humidity, oxygen gas pressure, carbon monoxide concentration, pressure, temperature, radiation, etc. For example, some humidity sensors are dependent on the p/n junction characteristics of a NiO/ZnO interface; oxygen gas sensors on the electronic conductivity properties of ZrO_2 ceramics; pressure sensors on the bulk piezoelectric properties of PZT ceramics (see Pressure measurements); and temperature sensors on the grain boundary characteristics of doped BaTiO_3 ceramics (see Temperature measurements).

The performance characteristics of ceramic sensors are defined by one or more of the following material properties: bulk, grain boundary, interface, or surface. Sensor response arises from the nonelectrical input because the environmental variable effects charge generation and transport in the sensor material.

Typical positive temperature coefficient (PTC) device behavior for a doped polycrystalline BaTiO_3 thermistor is presented in Figure 4. At temperatures below $\sim 100^\circ\text{C}$ and above $\sim 200^\circ\text{C}$ the material shows the expected negative resistivity vs temperature associated with semiconductors as expressed by:

$$\rho(T) = \rho_o \exp\left(\frac{-E_a}{kT}\right) \quad (5)$$

where $\rho(T)$ is the resistivity at temperature, T ; ρ_o is the pre-exponential factor; E_a is the activation energy for conduction; and k is the Boltzmann constant. This equation describes the thermal generation of carriers, or the increase in carrier mobility, which occurs over the temperature ranges where bulk transport phenomena

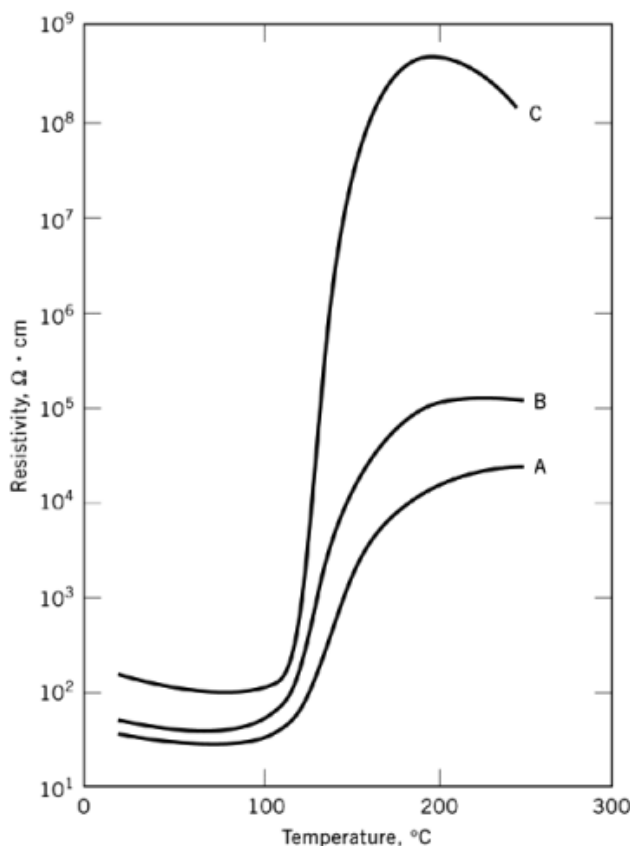


Fig. 4. Effect of dopant additions on the resistivity versus temperature behavior of BaTiO_3 PTCR ceramics. A, undoped; B, doped with 0.134 mol % Cr; and C, doped with 0.127 mol % Mn.

control conductivity. At temperatures between about 100 and 200°C, however, the resistivity increases by several orders of magnitude.

Because PTC thermistor compositions are generally processed under either reducing atmospheres or using La^{3+} or Y^{3+} (for Ba) dopant additions, donor states are generated in the grains, and these become semiconducting. At the grain boundaries acceptor states are formed through either acceptor impurity (Mn, Cr) segregation or chemisorption of oxygen during the annealing or cooling phase of the process cycle. This results in the formation of a potential barrier at the grain boundary. This barrier height increases with temperature above the Curie-Weiss temperature, and the increase in resistance, ie, the PTC effect, results. Because the acceptor doping level can affect the barrier height, the magnitude of the resistance increase that is observed in the vicinity of the Curie temperature can be controlled by dopant, as shown in Figure 4.

1.8. Varistors

Varistors are devices that exhibit nonlinear current–voltage behavior. At low voltages, current flow is minimal and the device behaves as an ohmic insulator. As the voltage approaches a critical value, the breakdown field (F_{BR}), current flow increases and the device becomes highly conducting. Because of this characteristic, varistors are typically employed as circuit overvoltage protection devices, ie, devices that protect solid-state circuitry

and other components against voltage spikes by diverting the current flow. The most frequently used material is doped zinc oxide, ZnO, which can handle both high current and high energy. Dopants include Sb_2O_3 , Bi_2O_3 , CoO , MnO , and Cr_2O_3 , present in quantities of ≤ 1 mol %. A typical composition is $96.5\text{ZnO}-0.5\text{Bi}_2\text{O}_3-1.0\text{CoO}-0.5\text{MnO}-1.0\text{Sb}_2\text{O}_3-0.5\text{Cr}_2\text{O}_3$.

Standard ceramic processing conditions are controlled so that the resulting ceramic microstructure is composed of semiconducting zinc oxide grains ($\rho_{\text{ZnO}} < 1\Omega\cdot\text{cm}$) and electrically insulating grain boundaries ($(\rho_{\text{gb}} > 10^6\cdot\text{cm})$). The microstructure is thus similar to that of the BaTiO_3 thermistor and device performance is dependent on the characteristics of the electrically insulating barriers at the grain boundaries, which result from trap states associated with the dopants (5, 10).

1.9. High Temperature Ceramic Superconductors

In 1986, it was reported that the compound $(\text{La}, \text{Ba})_2\text{CuO}_4$ displayed the transition to the superconducting state at a temperature of ~ 35 K. To be superconducting, a material must display two effects. First, it must display the Meissner effect at temperatures below T_c , the superconducting transition temperature. That is, the material must become diamagnetic and expel an externally applied magnetic field. Second, the electrical resistivity must decrease to zero at temperatures below T_c .

This extraordinary discovery of superconductivity in a ceramic material led to an explosion of research on other ceramic systems. The most notable include: $\text{YBa}_2\text{Cu}_3\text{O}_{7-\delta}$, $T_c \sim 93$ K; $\text{Bi}_2\text{CaSr}_2\text{Cu}_2\text{O}_x$, $T_c \sim 80$ K; and $\text{Tl}_2\text{Ca}_2\text{Ba}_2\text{Cu}_3\text{O}_y$, $T_c \sim 125$ K. Other bismuth- and thallium-based superconductors having different cation stoichiometries have also been discovered. The observed electrical properties of this family of ceramics are dependent on the crystallographic features and defect chemistry/oxygen stoichiometry of the materials (11). Because the superconducting properties of these compounds are a function of their oxygen content, a key aspect to processing is control of the oxygen partial pressure during heat treatment.

Ceramic, or oxide, superconductors (powders, thin films, and single crystals) have been prepared by a variety of techniques. Superconducting powders have been prepared by both traditional mixed oxide and chemical coprecipitation methods. The powders are processed into the desired form by techniques such as extrusion, pressing, or isostatic pressing. Thin films of the oxide superconductors have been prepared by a variety of sputtering techniques and chemical solution deposition approaches. Epitaxial growth and orientation of the films have been observed, and the fabrication of weak link Josephson junctions suitable for superconducting quantum interference devices (SQUIDS) has been reported (12). Finally, reasonably large single crystals of these materials have also been prepared. One technique that has been used extensively is flux growth, ie, growth from a molten salt bath.

2. Processing Techniques

2.1. Traditional Processing Routes

The majority of the electronic ceramics that are used for electronic applications crystallize in the perovskite structure. Many perovskite-type oxides can be prepared by conventional processing routes, ie, by high temperature solid-state reactions between the respective oxide powders. For example, to prepare the ABO_3 perovskite PZT, PbO , ZrO_2 , and TiO_2 are calcined at temperatures of $\sim 900^\circ\text{C}$ to induce crystallization into the desired structure. In addition to oxide precursors, carbonate powders of fine size may also be used to improve reaction kinetics and ensure a more complete reaction. For this process it is essential to remove the potential carbon contaminants during subsequent heat treatment. For materials having volatile constituents, such as the lead-based perovskite materials, additional measures are required to suppress, or compensate for, lead volatility during heat treatment. These include adding excess lead oxide to the initial batch, and/or carrying

10 CERAMICS, ELECTRONIC PROPERTIES AND MATERIAL STRUCTURE

out the calcination and sintering operations in a lead-rich atmosphere. Although processing to net-shape or near net-shape is desirable, a final machining step to yield a part of the exact size required is often necessary.

2.2. Chemical Coprecipitation of Powders

In the preparation of ceramics for such applications as piezoelectric transducers, traditional mixed oxide processing routes yield materials having acceptable properties. However, for the production of electrooptic ceramic components, deficiencies in the chemical homogeneity and optical properties prepared by these methods are frequently evident. Thus chemical methods of preparation, especially that of coprecipitation, are used to prepare powders for high quality defect-free optical devices. Because chemical methods of preparation are more costly than mixed oxide methods, the device requirements must necessitate the use of the more expensive processing techniques. Coprecipitation methods have been used extensively for the preparation of barium titanate, lanthanum-doped lead zirconate titanate (PLZT), and oxide superconductor powders.

In general, solution-based preparation methods involve dissolving precursor salts of the desired product, such as nitrates or chlorides, in a solvent, and subsequently recovering the cations that constitute that product. In terms of selecting the appropriate precursors, for multicomponent products such as PLZT, the mutual solubility of the various ingredients must be considered. The ability to dissolve several precursor salts in a mutual solvent allows for the preparation of homogeneous, multicomponent compositions, which is one of the most significant advantages of chemical coprecipitation. Other advantages include precise control of stoichiometry, the ability to uniformly disperse trace additives, freedom from contamination inherent in powder grinding and mixing operations, and because of the fine particle size of the resulting powders, higher reactivity and therefore lower sintering temperatures.

After preparing a homogeneous solution of the precursors, powder precipitation is accomplished through the addition of at least one complexing ion. For PLZT, frequently OH^- in the form of ammonium hydroxide is added as the complexing anion, which results in the formation of an amorphous, insoluble PLZT-hydroxide. Other complexing species that are commonly used are carbonate and oxalate anions. CO_2 gas is used to form carbonates. Irrespective of the complexing anion, the precipitated powders are eventually converted to the desired crystalline oxide phase by low temperature heat treatment.

A key aspect of the coprecipitation process is to ensure that the stoichiometry of the solution is maintained in the precipitated powder through quantitative precipitation of each of the cations in the material. In practice, this is accomplished by simultaneously exceeding the solubility product for each of the cations by adding the correct complexing anion(s) and controlling concentration variables. Theoretically, it is possible to control the precipitate size, size distribution, and morphology through an understanding of precipitation kinetics and control of precipitation variables such as reactor residence time.

Throughout subsequent processing the fine nature of the precipitated powders should be maintained. Minimizing agglomeration during solvent removal and calcination is thus an important aspect of downstream processing. Techniques such as freeze-drying or spray-drying are typically used during solvent removal. Subsequent component fabrication by pressing or other forming operations is similar to that used for powders prepared by the traditional mixed oxide process.

2.3. Solution Deposition of Thin Films

Chemical methods of preparation may also be used for the fabrication of ceramic thin films (qv). Metallo-organic precursors, notably metal alkoxides (see Alkoxides, metal) and metal carboxylates, are most frequently used for film preparation by sol-gel or metallo-organic decomposition (MOD) solution deposition processes (see Sol-gel technology). These methods involve dissolution of the precursors in a mutual solvent; control of solution characteristics such as viscosity and concentration, film deposition by spin-casting or dip-coating, and heat

treatment to remove volatile organic species and induce crystallization of the as-deposited amorphous film into the desired structure.

True sol-gel deposition routes have typically utilized solvents such as alcohols, and controlled additions of water to partially hydrolyze the metal alkoxide precursors and thus form polymeric solution species of higher molecular weight. The effects of varying the water to alkoxide molar ratio, and using acid and base catalysts to influence the hydrolysis and condensation reactions that lead to polymer formation are well understood for the silica system, but have been less extensively studied for multicomponent electronic ceramic systems, such as $\text{Pb}(\text{Zr}_{1-x}\text{Ti}_x)\text{O}_3$ and $\text{YBa}_2\text{Cu}_3\text{O}_{7-\delta}$. The effects of chemical modifiers such as chelating agents (qv), on the structures of solution polymeric species and their hydrolysis characteristics have been investigated.

Solution deposition processing has been used to prepare thin films (qv) of PbTiO_3 , PZT, PLT, PLZT, BaTiO_3 , LiNbO_3 , PMN, PMN-PT, PZN-PT, and $\text{YBa}_2\text{Cu}_3\text{O}_{7-\delta}$. For the preparation of PZT thin films, the most frequently used precursors have been lead acetate and zirconium and titanium alkoxides, especially the propoxides. Short-chain alcohols, such as methanol and propanol, have been used most often as solvents, although there have been several successful investigations of the preparation of PZT films from the methoxyethanol solvent system. The use of acetic acid as a solvent and chemical modifier has also been reported. Whereas PZT thin films with excellent ferroelectric properties have been prepared by sol-gel deposition, there has been relatively little effort directed toward understanding solution chemistry effects on thin-film properties.

2.4. Alternative Thin-Film Fabrication Approaches

Thin films of electronic ceramic materials have also been prepared by sputtering, electron beam evaporation, laser ablation, chemical beam deposition, and chemical vapor deposition (CVD). In the sputtering process, targets may be metal (elemental), single-phase oxide, or mixed-phase pressed powder targets. In the preparation of PZT and PLZT thin films, multitarget sputtering using elemental targets or single component oxide targets has been utilized.

3. Other Applications

3.1. Diamond and Refractory Ceramic Semiconductors

Ceramic thin films of diamond, silicon carbide, and other refractory semiconductors (qv), eg, cubic BN and BP and GaN and GaAlN, are of interest because of the special combination of thermal, mechanical, and electronic properties (see Refractories). The majority of the research effort has focused on SiC and diamond, because these materials have much greater figures of merit for transistor power and frequency performance than Si, GaAs, and InP (13). Compared to typical semiconductors such as Si and GaAs, these materials also offer the possibility of device operation at considerably higher temperatures. For example, operation of a silicon carbide MOSFET at temperatures above 900 K has been demonstrated. These devices have not yet been commercialized, however.

3.2. Ferroelectric Thin-Film Devices

Since 1989, the study of ferroelectric thin films has been an area of increasing growth. The compositions studied most extensively are in the PZT/PLZT family, although BaTiO_3 , KNbO_3 , and relaxor ferroelectric materials, such as PMN and PZN, have also been investigated. Solution deposition is the most frequently utilized fabrication process, because of the lower initial capital investment cost, ease of film fabrication, and the excellent dielectric and ferroelectric properties that result.

Numerous uses for PZT/PLZT thin films are under investigation. The device that, as of this writing, is closest to commercialization is a nonvolatile memory. This device, which utilizes a ferroelectric thin-film capacitor integrated onto silicon circuitry, provides memory retention when the power is off because of the

12 CERAMICS, ELECTRONIC PROPERTIES AND MATERIAL STRUCTURE

polarization retention of the ferroelectric capacitor. One and zero memory states arise from the two polarization states, $-P_R$ and $+P_R$, of the ferroelectric. Because PZT is radiation-hard, the devices are also of interest for military and space applications.

Decoupling capacitors and dynamic random access memories (DRAMs), are based on the dielectric properties of these materials. Applications based on the electrooptic properties include total internal reflection (TIR) switches, optical interconnects, waveguides, optical image comparators, and optical storage disks (see Information storage materials). One of the earliest demonstrations of an optical device was in 1984 (14), when the high speed TIR switching behavior of sputter-deposited PLZT thin films was recognized. Use of these materials as optical storage media has also been investigated. In 1989, photosensitivity and electrooptic coefficients of PZT and PLZT thin films was reported (15). A device configuration suitable for optical information storage was proposed.

BIBLIOGRAPHY

Cited Publications

1. L. L. Hench and J. K. West, *Principles of Electronic Ceramics*, John Wiley & Sons, Inc., New York, 1990.
2. E. N. Bunting, G. R. Shelton, and A. S. Creamer, *J. Res. Natl. Bur. Std.* **38**, 337–349 (1947).
3. L. F. Francis, *Sol-Gel Processing, Perovskite Phase Development and Properties of Relaxor-Based Thin-Layer Ferroelectrics*, Ph.D. dissertation, University of Illinois, Urbana, 1991.
4. G. H. Haertling, “Piezoelectric and Electrooptic Ceramics,” in R. C. Buchanan, ed., *Ceramic Materials for Electronics*, Marcel Dekker, Inc., New York, 1986.
5. A. J. Moulson and J. M. Herbert, *Electroceramics*, Chapman & Hall, New York, 1990.
6. H. F. Kay and P. Vousden, *Phil Mag.* **40**, 1019–1040 (1949).
7. W. J. Merz, *Phys Rev.* **76**, 1221–1225 (1949).
8. R. W. Whatmore, *Ferroelectrics* **49**, 201–210 (1983).
9. A. Goldman, *Am. Ceram. Soc. Bull.* **63**, 582–585, 590 (1984).
10. L. Levinson and H. R. Philipp, “Application and Characterization of ZnO Varistors,” in Ref. 4.
11. K. Kitazawa, *Am. Ceram. Soc. Bull.* **68**(4), 880–882 (1989).
12. K. Char, M. S. Colclough, S. M. Garrison, N. Newman, and G. Zaharchuk, *Appl. Phys. Lett.* **59**(6), 733–735 (1991).
13. R. F. Davis, *Int. J. Mater. Product Tech.* **4**(2), 81–103 (1989).
14. K. Wasa, O. Yamazaki, H. Adachi, T. Kawaguchi, and K. Setsune, *J. Lightwave Tech.* **LT-2**(5), 710–714 (1984).
15. C. E. Land, *J. Am. Ceram. Soc.* **72**(11), 2059–2064 (1989).

General References

16. H. Adachi, T. Mitsuyu, O. Yamazaki, and K. Wasa, *Jpn. J. Appl. Phys.* **24**(Suppl. 24–3), 13–16 (1985).
17. A. Bologna Alles, V. R. W. Amarakoon, and V. L. Burdick, *J. Am. Ceram. Soc.* **72**(1), 148–151 (1989).
18. J. R. Belsick, A. Halliyal, U. Kumar, and R. E. Newnham, *Am. Ceram. Soc. Bull.* **66**(4), 664–667 (1987).
19. D. Bondurant and F. Gnadinger, *IEEE Spectrum* **26**(7), 30–33 (1989).
20. U.S. Pat. 4,839,339 (1989), B. C. Bunker, D. L. Lamppa, and J. A. Voigt.
21. A. T. Collins, *Semicond. Sci. Technol.* **4**, 605–611 (1989).
22. L. E. Cross, *Am. Ceram. Soc. Bull.* **63**(4), 586–590 (1984).
23. L. E. Dolhert and co-workers, *Int. J. Hybrid. Microelectronics* **14**(4), 113–120 (1991).
24. *Phys. Today*, 55–62 (Jan. 1987).
25. G. Fisher, *Am. Ceram. Soc. Bull.* **63**(4), 569–571 (1984).
26. G. Fisher, *Am. Ceram. Soc. Bull.* **66**(4), 622–624, 626–629 (1987).

27. G. Fisher, *Am. Ceram. Soc. Bull.* **67**(4), 725–735 (1988).
28. J. R. Gaines, Jr., *Am. Ceram. Soc. Bull.* **68**(4), 857–859 (1989).
29. A. Halliyal, U. Kumar, R. E. Newnham, and L. E. Cross, *Am. Ceram. Soc. Bull.* **66**(4), 671–676 (1987).
30. A. H. Hamdi and co-workers, *Appl. Phys. Lett.* **53**(5), 435–437 (1988).
31. L. C. Hoffman, *Am. Ceram. Soc. Bull.* **63**(4), 572–576 (1984).
32. L. Ketron, *Am. Ceram. Soc. Bull.* **68**(4), 860–865 (1989).
33. M. Kojima, M. Okuyama, T. Nakagawa, and Y. Hamakawa, *Jpn. J. Appl. Phys.* **22**(Suppl. 22–2), 14–17 (1983).
34. A. H. Kumar and R. R. Tummala, *Int. J. Hybrid Microelectron.* **14**(4), 137–150 (1991).
35. N. Kuramoto, H. Taniguchi, and I. Aso, *Am. Ceram. Soc. Bull.* **68**(4), 883–887 (1989).
36. L. Levinson and H. R. Philipp, *Am. Ceram. Soc. Bull.* **65**(4), 639–646 (1986).
37. L. M. Levinson, *Am. Ceram. Soc. Bull.* **68**(4), 866–868 (1989).
38. K. K. Likharev, V. K. Semenov, and A. B. Zorin, “New Possibilities for Superconducting Devices,” in S. T. Ruggiero and D. A. Rudman, eds., *Superconducting Devices*, Academic Press, Inc., New York, 1990.
39. K. S. Mazdiasni, *Am. Ceram. Soc. Bull.* **63**(4), 591–594 (1984).
40. S. J. Milne and S. H. Pyke, *J. Am. Ceram. Soc.* **74**(6), 1407–1410 (1991).
41. M. Naito, *Ceram. Eng. Sci. Proc.* **8**(9–10), 1106–1119 (1987).
42. L. H. Parker and A. F. Tasch, *IEEE Circuits Devices Mag.*, 17–26 (Jan. 1990).
43. J. D. Parsons, R. F. Bunshah, and O. M. Stafsudd, *Sol. St. Tech.*, 133–139 (Nov. 1985).
44. I. G. Sarda and W. H. Payne, *Am. Ceram. Soc. Bull.* **67**(4), 737–746 (1988).
45. B. Schwartz, *Am. Ceram. Soc. Bull.* **63**(4), 577–581 (1984).
46. J. F. Scott and C. A. Paz de Araujo, *Science* **246**, 1400–1405 (1989).
47. L. M. Sheppard, *Adv. Mater. Process.*, 19–25 (Sept. 1986).
48. T. R. Shrout and A. Halliyal, *Am. Ceram. Soc. Bull.* **66**(4), 704–711 (1987).
49. R. R. Tummala, *Am. Ceram. Soc. Bull.* **67**(4), 752–758 (1988).
50. B. A. Tuttle, *Mater. Res. Soc. Bull.* **12**(7), 40–45 (1987).
51. R. W. Vest and J. Xu, *Ferroelectrics* **93**, 21–29 (1989).
52. R. W. Whatmore, A. Patel, N. M. Shorrocks, and F. W. Ainger, *Ferroelectrics* **104**, 269–283 (1990).
53. G. Yi, Z. Wu, and M. Sayer, *J. Appl. Phys.* **64**(5), 2717–2724 (1988).

ROBERT SCHWARTZ
Sandia National Laboratories

Related Articles

Ceramics as electrical materials; Ceramics, Overview; Ceramics, Ceramic Processing; Ceramics, Mechanical Properties and Behavior; Ceramics, Glass Structure and Properties; Ceramics, Nonlinear Optical and Electrooptic Ceramics